



# Collagen based magnetic nanocomposites for oil removal applications

Palanisamy Thanikaivelan<sup>1,2</sup>, Narayanan T. Narayanan<sup>1</sup>, Bhabendra K. Pradhan<sup>3</sup> & Pulickel M. Ajayan<sup>1</sup>

<sup>1</sup>Department of Mechanical Engineering and Materials Science, Rice University, Houston, TX 77005, USA, <sup>2</sup>Advanced Materials Laboratory, Center for Leather Apparel & Accessories Development, Central Leather Research Institute (Council of Scientific and Industrial Research), Adyar, Chennai 600020, India, <sup>3</sup>Nanoholdings LLC, 360 Bloombridge Way, Marietta, GA 30066, USA.

SUBJECT AREAS:

SUSTAINABILITY

MATERIALS

NANOBIOTECHNOLOGY

MAGNETIC MATERIALS AND  
DEVICES

Received

7 November 2011

Accepted

2 January 2012

Published

20 January 2012

Correspondence and requests for materials should be addressed to P.T. (thanik8@yahoo.com) or P.M.A. (ajayan@rice.edu)

**A stable magnetic nanocomposite of collagen and superparamagnetic iron oxide nanoparticles (SPIONs) is prepared by a simple process utilizing protein wastes from leather industry. Molecular interaction between helical collagen fibers and spherical SPIONs is proven through calorimetric, microscopic and spectroscopic techniques. This nanocomposite exhibited selective oil absorption and magnetic tracking ability, allowing it to be used in oil removal applications. The environmental sustainability of the oil adsorbed nanobiocomposite is also demonstrated here through its conversion into a bi-functional graphitic nanocarbon material via heat treatment. The approach highlights new avenues for converting bio-wastes into useful nanomaterials in scalable and inexpensive ways.**

Composites prepared from biopolymers of natural or biological origin have received much attention in recent times. Combination of nanoparticles and biodegradable polymers can yield nanobiocomposites, which have the potential for various biomedical and environmental applications<sup>1–3</sup>. Though the biocompatibility of many nanoparticles is questionable<sup>4,5</sup>, magnetic iron oxide ( $\text{Fe}_3\text{O}_4/\gamma\text{Fe}_2\text{O}_3$ ) is proven for its low degree of cytotoxicity even with considerably high loadings<sup>6,7</sup>. This makes iron oxide nanoparticles as an ideal magnetic material for bio-diagnostics and imaging. Collagen is a widely available biodegradable fibrous protein with a triple helical structure<sup>8</sup>. Significant amount of collagen containing wastes are generated from protein processing industries such as slaughter house, meat packing, leather and related industries. Leather industry dominates among them in generating voluminous pure as well as tainted collagen wastes amounting up to 600 kg per ton of skins/hides processed<sup>9</sup>. Although many ways of utilizing these wastes have been attempted<sup>10</sup>, development of new multifunctional materials of high value is gaining importance. Collagen being a protein tends to destabilize on exposure to heating or specific enzymes such as collagenase. Hence, collagen needs to be stabilized for its widespread applications in fields such as leather making, tissue engineering and cosmetics. Variety of metals including chromium has been tested for their ability to stabilize the collagen fibers through molecular interactions and structural modifications. Only a few of them seem to permanently stabilize the collagen matrix and improve its hydrothermal stability<sup>11–13</sup>. Interaction of nanoparticles with collagen fibers is an upcoming and stimulating research area<sup>14,15</sup>. Aqueous suspensions of magnetic  $\text{Fe}_3\text{O}_4$  nanoparticles<sup>16–18</sup> of uniform particle size ( $\sim 10$  nm), known as ferrofluid (FF), could be an interesting candidate for exploiting such interactions.

Used or spent oils are toxic to the microflora present in the marine environment as well as effluent treatment plants<sup>19</sup>. Besides, oil spill in the ocean or water bodies forms a major environmental threat to the aquatic life forms all over the world<sup>20</sup>. The use of floating barriers is the most commonly used technique to control the spread of oil, whereas sorbents are used to remove final traces of oil, or in areas that cannot be reached by skimmers. Adebajo and colleagues<sup>21</sup> reviewed extensively on the variety and efficiency of known oil absorbents. They include three major classes, namely, inorganic, synthetic organic and natural organic products with oil absorption capacity as low as 0.5 times to as high as 237 times of their weight. Inorganic products include zeolites, silica, perlite, graphite, vermiculites, clay and diatomite. Synthetic organic products include acrylates<sup>22</sup>, butyl rubber<sup>23</sup>, polydimethylsiloxane<sup>24</sup>, polypropylene and polyurethane foams<sup>25</sup>. Some of them are the most commonly used commercial sorbents in oil spill cleanup although they degrade very slowly<sup>21</sup>. Natural organic sorbents that have been reported include straw, corn cob, wood fiber, cotton fiber, leather fibers<sup>26</sup>, cellulosic kapok fiber, kenaf, milkweed floss and peat moss. Recently, advanced materials are being developed to selectively absorb oil with additional functionality<sup>19,20,27–29</sup>. However, they have limitations such as difficult preparation steps, small particle size, low separation efficiency, and cost<sup>27</sup>.



Here, we have utilized aqueous superparamagnetic iron oxide ( $\text{Fe}_3\text{O}_4$ ) nanoparticles to stabilize the collagen waste fibers (Fig. 1a) for selectively removing oil from water by magnetic tracking. Furthermore, the oil absorbed magnetic nanobiocomposite has been converted into bi-functional carbon materials that can be used for a variety of applications, providing a sustainable cycle for waste recycling and environmental cleanup.

## Results

**Stabilization of waste collagen fibers using SPION.** Wet collagen-SPION nanobiocomposite and pristine collagen wet fibers were analyzed using differential scanning calorimeter (Fig. 1b) to understand their hydrothermal stability. Collagen is known to shrink irreversibly around  $65^\circ\text{C}$  when heated in water, which is known as shrinkage temperature or hydrothermal stability<sup>13</sup>. It is seen that the hydrothermal stability of the native collagen is increased up to  $86.8^\circ\text{C}$  after reacting with SPION. This may be due to the interaction between citric acid coated on the  $\text{Fe}_3\text{O}_4$  nanoparticles and side chain amino functional groups of collagen molecules present in the penta-fibril assembly (Fig. 1a). Since the size of  $\text{Fe}_3\text{O}_4$  nanoparticles is 10 nm, it can only interact with the collagen molecules in the periphery of penta-fibril assembly. In other words, it may not enter the nano pores present in the penta-fibril assembly unlike chromium ions used for collagen stabilization. The observed hydrothermal stability is on par with the values reported for the collagen stabilization achieved by the use of metal salts such as titanium, zirconium, aluminium, iron, zinc or plant derived polyphenols<sup>12,13,30</sup> or silica nanoparticles<sup>31</sup>. Figure 1c shows the x-ray diffraction patterns of pristine collagen fibers and collagen-SPION nanobiocomposite. It is seen that the intermolecular lateral packing (peak 1) reduces to a

greater extent when the SPION interacted with collagen indicating that the collagen packing order decreases. This may be due to the introduction of cross-linking between collagen molecules and SPION leading to the decreased order in collagen organization. Such kind of reduction has been observed earlier when collagen was treated with chromium(III) ions<sup>32</sup>. The collagen structural details as calculated from XRD data are given in Supplementary Table S1 online. Most of the characteristic peaks of collagen appear to be relatively unchanged upon treatment with SPION. However, it is seen that the collagen to amorphous ratio seems to be decreased for the composite, which is attributed to the SPION and collagen interaction. It is calculated by dividing the slope of peak 1 by the slope of peak 2 corresponding to amorphous region<sup>33</sup>. Nevertheless, such reduction does not lead to gelatinization, which is the complete loss of structural order of collagen. Micro-Raman spectra of the pristine collagen fibers and collagen-SPION nanobiocomposite further confirm that the interaction between SPION and collagen fibers does not alter or destroy the principal triple helical structure of collagen (see Supplementary Fig. S1 online). X-ray photoelectron spectroscopy results provide sufficient evidence for the presence of iron(III) nanoparticles in the synthesized collagen-SPION nanobiocomposite (see Supplementary Fig. S2 online).

**Morphology of collagen-SPION nanobiocomposite.** Figure 2a shows the FESEM image of pristine collagen fibers. The inset, magnified image of the select portion, shows the banded structure with a characteristic D-periodicity of  $\sim 64 \pm 1$  nm reflective of quarter staggered arrangement of collagen molecules into a penta-fibril assembly. This is in good agreement with the earlier observations on pristine collagen fibers<sup>34</sup>. FESEM of collagen-SPION nanobiocomposite as

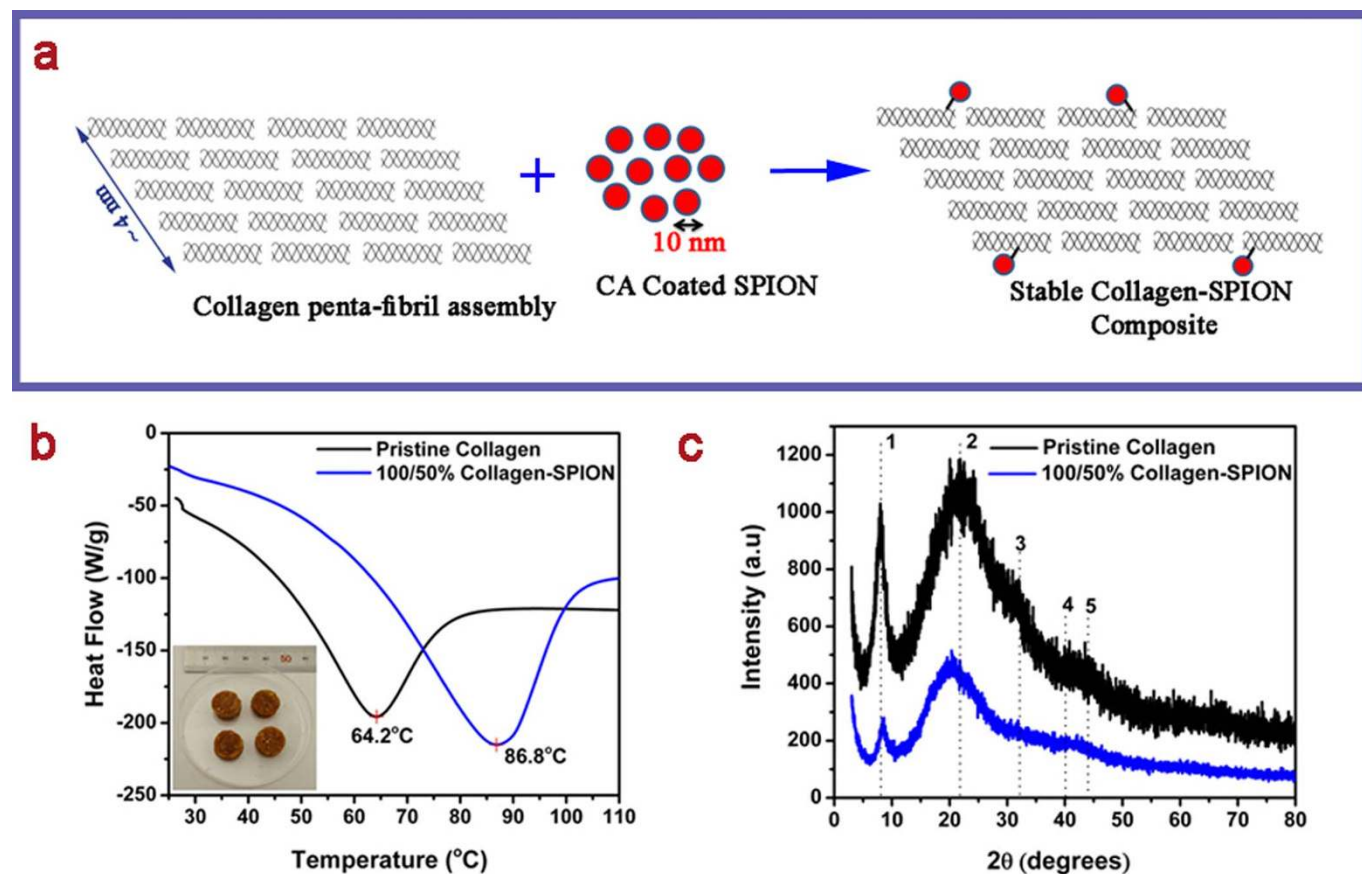


**Figure 1 | Stabilization of collagen waste fibers using SPION.** (a) Schematic showing the interaction of collagen waste fibers and SPION nanoparticles to yield collagen-SPION nanobiocomposite (ratio of collagen and SPION by weight is 100/50%; figure (a) not drawn to scale); (b) DSC traces of pristine collagen and collagen-SPION nanobiocomposite, in the figure Endo down (inset shows the photograph of collagen-SPION composite pellet with 10 mm dia); (c) XRD patterns of pristine collagen and collagen-SPION nanobiocomposite.

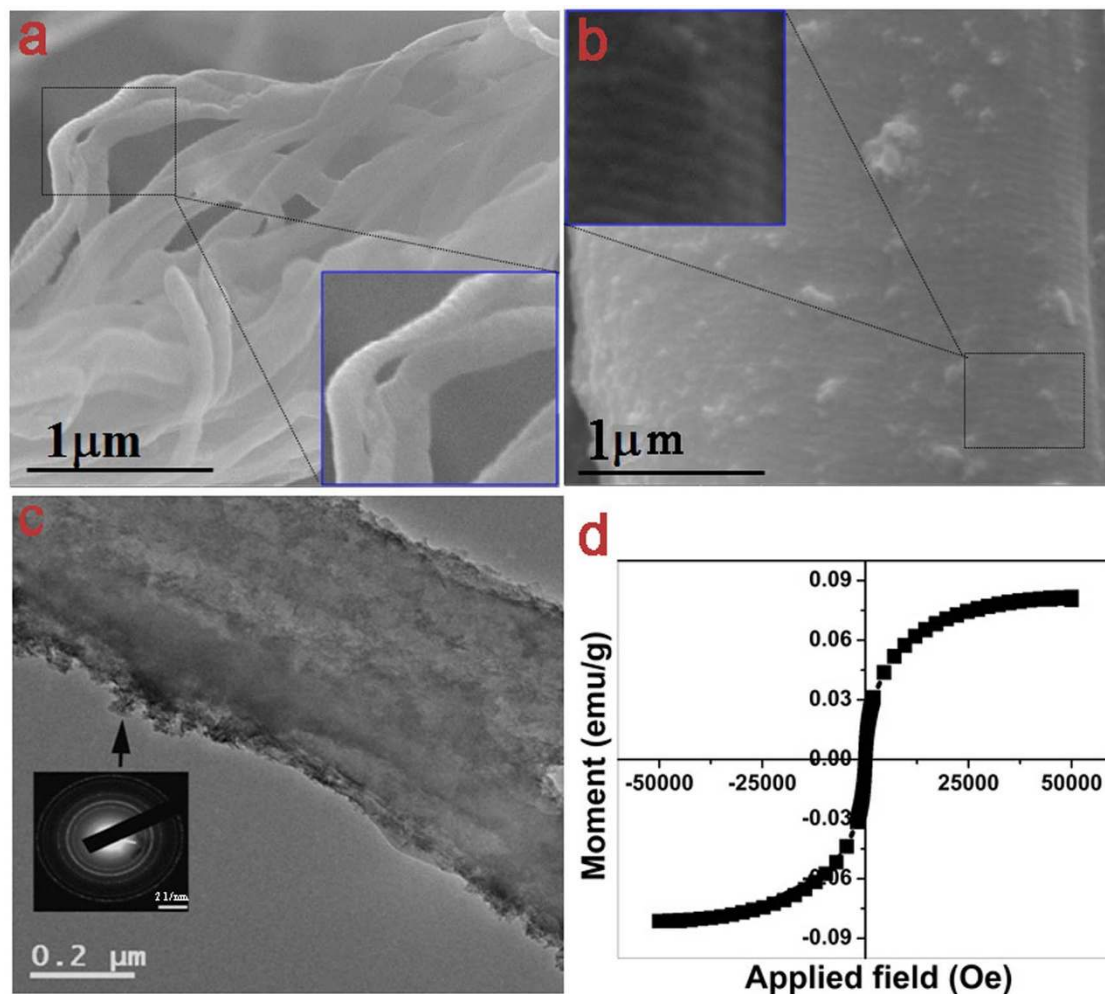


**Figure 2 | Morphology and magnetism of collagen-SPION nanobiocomposite.** FESEM showing (a) collagen waste fibers (b) collagen waste-SPION nanobiocomposite fiber bundle. Insets show the magnified view of the select portion exhibiting the bands of collagen fibers; (c) TEM of collagen waste-SPION nanobiocomposite fiber showing the SPION coated on the collagen fiber. SAED shows the crystalline nature of the SPION; (d) SQUID of collagen waste-SPION nanobiocomposite showing superparamagnetism.

shown in Fig. 2b demonstrate the attachment of SPION nanoparticles to the collagen fibers. It is seen that the collagen banding persists even after interaction with SPION nanoparticles, however, the D-periodicity is markedly reduced to  $\sim 59 \pm 1$  nm. This may be due to the dense packing of collagen molecules by the displacement of water molecules<sup>35</sup> owing to the interaction of SPION nanoparticles and collagen penta-fibrillar assembly. Such reduction in collagen D-periodicity has been reported earlier for the interaction between collagen matrix and dimeric chromium(III) complexes<sup>36</sup> and shown as an evidence for the stabilization of collagen from degradation. TEM image shows a nonconformal coating of SPION nanoparticles on the surface of collagen fibers (Fig. 2c). The inset shows the SAED pattern of SPIONs from the marked area of the composite. It shows that SPIONs are nanocrystalline (diffused rings) and has spinel structure. This is interesting since the collagen itself is an amorphous molecule (see Supplementary Fig. S3 online for SAED pattern of collagen portion in the TEM). The room temperature magnetization measurement of the composite shows (Fig. 2d) a typical superparamagnetic S-like curve. Zero coercivity and remanence of the nanobiocomposite indicates that SPIONs (here  $\text{Fe}_3\text{O}_4$ ) are not interacting with each other though they are individually bound to collagen waste fibers.

**Application of collagen-SPION nanobiocomposite for oil removal.** The obtained magnetic collagen nanocomposites were dried and used to absorb and selectively remove oil from oil-water

mixture. The magnetic nanocomposites were added to the used motor oil-water mixture in a Petri dish and allowed to absorb oil. The different steps of the oil absorption are shown in Figure 3a–c. It is also possible to utilize the magnetic property of the synthesized nanobiocomposite to track and absorb more oil in other oil contaminated area under magnetic field. To demonstrate this, a permanent magnet (field  $\sim 2000$  Oe) was used to track the magnetic nanobiocomposite such that it can absorb more oil effectively from all over the surface of used motor oil-water mixture in the Petri dish (see Supplementary Movie S1 online). It should be noted that the magnetic field was applied above the water-oil surface. Two oils were chosen namely premium motor oil and used motor oil in order to assess the oil absorbing capacity of the derived magnetic nanobiocomposite. It has been found that the maximum oil sorption capacity of the synthesized magnetic nanobiocomposite is about 2 g/g for the used motor oil (similar to that of some commercially available polymers), as shown in Fig. 3d. This was achieved quasi-instantaneously within few minutes. Further, it may be possible to improve the oil sorption capacity of the derived nanobiocomposite, if one can employ critical point drying to increase the surface area instead of normal drying.

## Discussion

Conventional methods of collagen stabilization predominantly employ either chromium(III) ions or plant derived polyphenolic

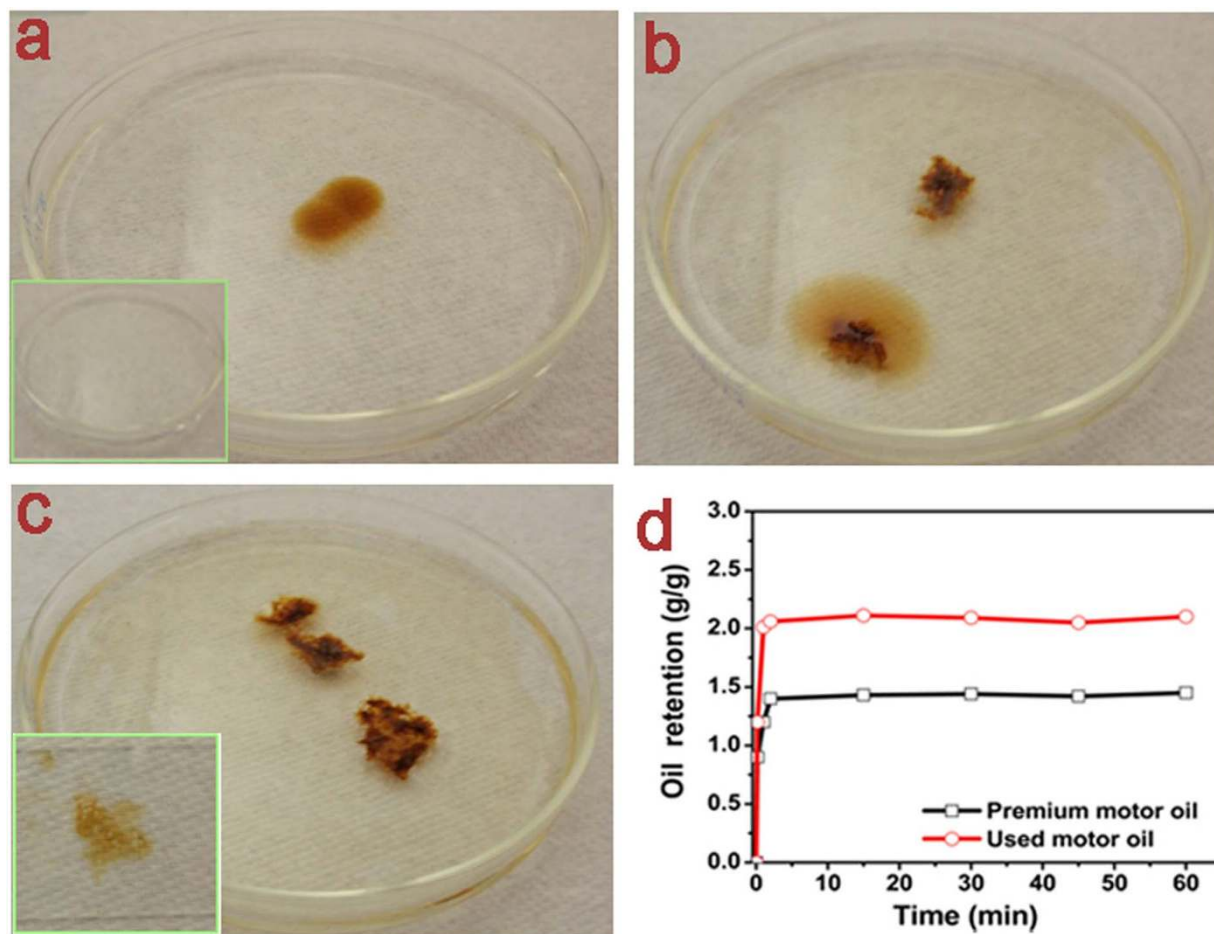


**Figure 3 | Oil removal using collagen-SPION nanobiocomposite.** (a) Oil in water medium placed in a Petri dish. Inset shows the pure water; (b) Collagen-SPION nanobiocomposite is added on the oil; (c) Collagen-SPION nanobiocomposite after oil absorption. Inset shows the squeezed oil from oil-absorbed collagen-SPION nanobiocomposite; (d) Oil retention ability of the collagen-SPION nanobiocomposite as a function of time using premium and used motor oil.

compounds (vegetable tannins). While chromium(III) ions irreversibly bind with collagen carboxyl groups through coordinate covalent bonding leading to high thermal stability ( $\sim 120^{\circ}\text{C}$ ), vegetable tannins offer moderate collagen stabilization ( $\sim 80^{\circ}\text{C}$ ) through physical deposition, hydrogen bonding as well as electrostatic interactions<sup>13</sup>. Here, the  $\text{Fe}_3\text{O}_4$  nanoparticles have been shown to stabilize the collagen fibers appreciably ( $\sim 87^{\circ}\text{C}$ ) through differential scanning calorimetric analysis (Fig. 1b). The use of DSC for measuring the thermal stability of collagen is well known, however, selection of heating rate is critical as higher heating rate may not show exact phase transition during thermal shrinkage<sup>37</sup>. Here, we have used a slow heating rate ( $2^{\circ}\text{C}$ ), which was sufficient to discern the shrinkage process. The observed shrinkage temperature of the collagen-SPION nanobiocomposite could be due to electrostatic interactions between citric acid coated on the  $\text{Fe}_3\text{O}_4$  nanoparticles and side chain amino functional groups of collagen molecules as well as physical deposition as later verified using SEM and TEM investigations (Fig. 2a–c). These results suggest that the SPION induced stabilization of collagen is analogous to the mechanisms proposed for the interaction between collagen and vegetable tannin. Although the use of nanomaterials for the stabilization of collagen is not new, achieving stable and multifunctional collagen matrix is a challenging proposition. In this study, we have synthesized such a stable, cheap and magnetic nanocomposite using collagen waste fibers and SPION for several applications including selective oil removal (Fig. 3a–c) and tracking under magnetic field. The normally dried collagen-SPION nanobiocomposite is capable of absorbing oil up to 2 times its own weight (Fig. 3d) and this

is comparable to the existing absorbent materials currently available in the market, for example, a Smart Sponge® developed and marketed by AbTech Industries<sup>38</sup>. However, it should be noted that the collagen-SPION nanobiocomposite developed here not only able to absorb oil selectively but also be mobilized or tracked under magnetic field (see Supplementary Movie S1 online), which was applied above the water surface. The plausible mechanism for the oil absorption in this study is that the collagen in the collagen-SPION nanobiocomposite was absorbing the oil. SPIONs are not only used for magnetic tracking purpose but also for stabilizing the collagen waste fibers for industrial applications including oil removal. Such low-cost and multifunctional nanocomposites capable of absorbing oil have not been reported so far.

Considering that we have utilized an industrial waste to remove another waste, it is imperative to look at the fate of final product namely oil absorbed nanobiocomposite. Although one can mechanically squeeze and remove the oil and reuse further for oil absorption, the recycling process generally can not exceed a maximum of 10 or 20 cycles and one need to look for disposal options. Hence, we propose to convert this oil absorbed nanobiocomposite into useful nanocarbon materials (Fig. 4a) via simple heat treatment in anoxic conditions (Fig. 4b); for example,  $1000^{\circ}\text{C}$  for 2 h. TEM image of the carbon derived from oil absorbed nanobiocomposite shows iron oxide nanoparticles, with  $\geq 30$  nm size, embedded in dense layers of carbon matrix (Fig. 4c). It seems that the iron oxide nanoparticles are not directionally grown as evidenced from SAED pattern in the inset. The presence of (002) and (101) diffraction peaks in the XRD pattern

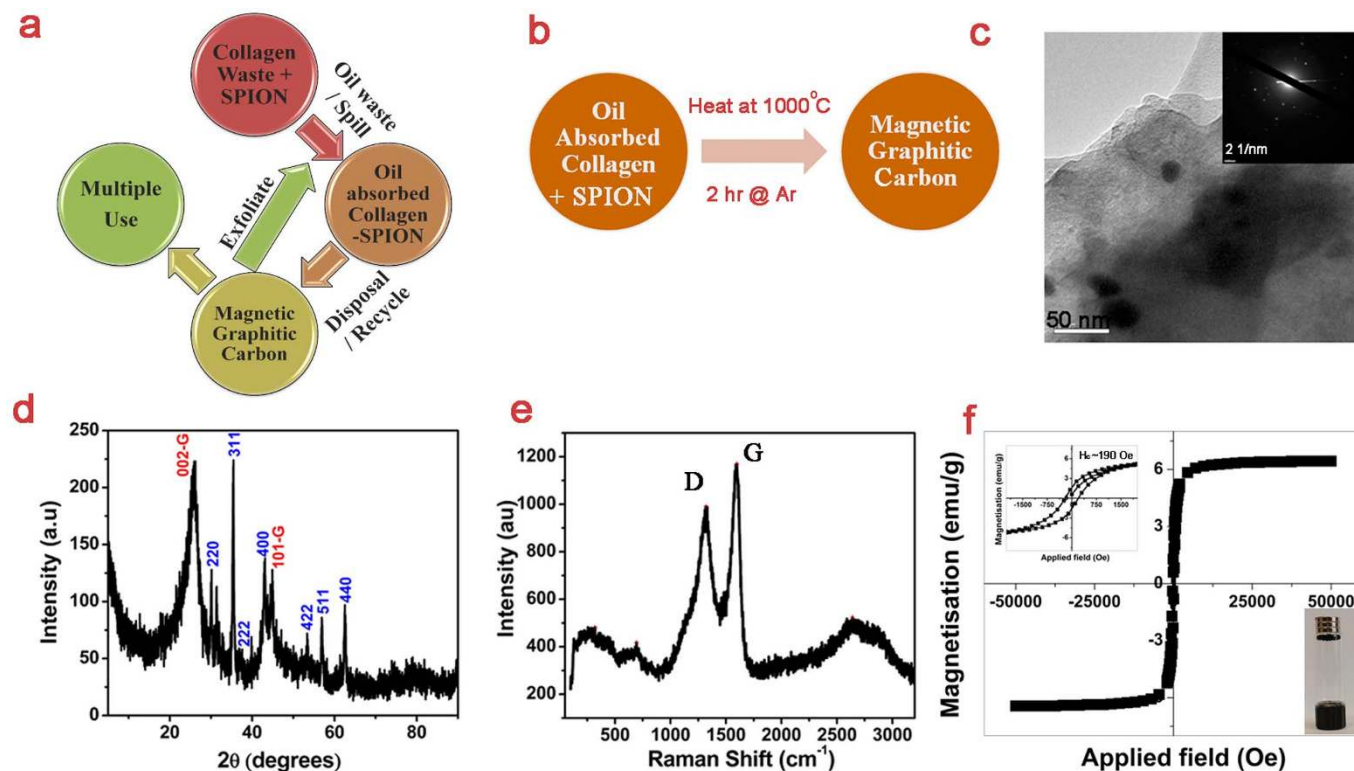


**Figure 4** | Transforming oil absorbed nanobiocomposite into bi-functional nanocarbon material. (a) Schematic showing the complete lifecycle of the proposed process on the utilization of collagen wastes; (b) Schematic showing a simple heat treatment to convert oil absorbed nanobiocomposite into magnetic and conducting graphitic carbon; (c) TEM image of graphitic carbon derived from oil absorbed nanobiocomposite. Inset shows the SAED pattern of the iron oxide nanoparticles inside the carbon layers; (d) XRD pattern, (e) Raman spectra and (f) SQUID of the derived graphitic carbon. Inset in (f) shows more amount of graphitic carbon samples are trapped on the top of the glass vial against the force of gravity under permanent magnets ( $\sim 500$  Oe).

demonstrates the graphitization and high crystallinity of the derived carbon materials (Fig. 4d). In addition, it is also seen that diffraction peaks of iron oxide nanoparticles are overlapping with the graphitic carbon peaks. The positions of all the indexed diffraction peaks except graphitic peaks matched well with that of  $\text{Fe}_3\text{O}_4$  (JCPDS 85-1436). Raman spectra of the carbon derived from oil absorbed nanobiocomposite shows peaks corresponding to D, G and 2D modes of  $\text{sp}^2$  bonded carbon atoms in two-dimensional hexagonal graphitic lattice (Fig. 4e). The broad band around  $2700\text{ cm}^{-1}$  (2D mode) suggests exfoliation of graphene layers in the derived graphitic carbon. The  $I_G/I_D$  ratio of the derived carbon is 1.18 indicating the presence of structural defects primarily due to the multiple graphitic layers as well as the presence of non-carbon atoms<sup>39,40</sup>. The observance of broad peaks around  $\sim 320$  and  $700\text{ cm}^{-1}$  may be attributed to the hematite and magnetite phases of iron oxide, respectively<sup>41</sup>. However, it seems that the magnetite phase of iron oxide is higher in the derived graphitic carbon as evidenced from XRD results. XPS results show the presence of oxygen and nitrogen functionalities thereby demonstrating the self-doping of the synthesized carbon derived from oil absorbed nanobiocomposite (see Supplementary Fig. S4 online). However, it could only show traces of iron due to the fact that the  $\text{Fe}_3\text{O}_4$  nanocrystals are embedded in the carbon matrix and XPS can perform only a surface analysis. The atomic concentration of the derived carbon as calculated from XPS was 85.3, 13.5, 1.1 and 0.1% of C, O, N and Fe, respectively. It is interesting to note that the SQUID result of the derived carbon (Fig. 4f) is distinct from the initial collagen-SPION nanobiocomposite. The  $M(H)$  loop has been opened and it depicts a coercivity of  $\sim 190$  Oe as seen from the inset of Fig. 4f, showing a perfect ferrimagnetic property with saturation magnetization. This indicates that crystal growth occurred during the heat treatment and particle size of  $\text{Fe}_3\text{O}_4$  is enhanced. This is in

agreement with the TEM observations (Fig. 4c). Moreover, the nature of SAED is also changed from nanocrystalline diffused spots corresponding to initial SPIONs in the nanobiocomposite to crystalline spots. This further evidences the growth of  $\text{Fe}_3\text{O}_4$  nanocrystals in the carbon matrix during the heat treatment thereby causing a paradigm shift from superparamagnetic to ferrimagnetic nanoparticles. The synthesized conductive (bulk electrical resistance of the as-synthesized carbon is  $\sim 1\text{ k}\Omega$ ) and magnetic graphitic carbon can find numerous applications in various fields including oil removal, energy storage and biomedicine. It has been earlier shown that exfoliated graphite can act as a sorbent for oil removal applications<sup>20</sup>. It has also been shown that core-shell  $\text{Fe}_2\text{O}_3@\text{C}$  nanoparticles can be used to remove oil under magnetic field<sup>27</sup>. It can be reckoned that our magnetic graphitic carbon ( $\text{Fe}_3\text{O}_4$  nanocrystals embedded in the carbon matrix) is logically similar to that of the previous report. Hence, our bi-functional graphitic carbon can be used for oil removal as well as magnetic tracking with or without exfoliation (Fig. 4a).

In summary, we demonstrated the stabilization of collagen waste fibers using superparamagnetic  $\text{Fe}_3\text{O}_4$  nanoparticles suspended in aqueous medium. Apart from possible industrial requirement of stabilized collagen matrix, we showed the oil absorption and magnetic tracking efficiency of this stable nanobiocomposite. Further, we converted the oil absorbed nanocomposite into a magnetic graphitic carbon material, which can have potential applications in several areas.

## Methods

**Synthesis, application and environmental sustainability of magnetic nanobiocomposites from collagen wastes.** Collagen wastes in the form of bovine hide trimming pieces, area ranging from 25 to  $300\text{ cm}^2$ , were collected from a local tannery at Chennai. The trimming pieces were soaked, limed, dehaired, relimed,



fleshed and delimed completely using conventional procedures<sup>42,43</sup> to remove hair, flesh and unwanted non-collagenous proteins. The delimed hide pieces were soaked in 35 and 70% acetone followed by 100% methanol for sufficient duration. This final step was repeated five times in order to completely remove the moisture. Finally, the hide pieces were thoroughly dried in a vacuum drier. The completely dried hide pieces were grounded finely into powder using a Willy mill of mesh size 2 mm. The obtained dry hide powder can be stored in a closed plastic bag for several months. Fe<sub>3</sub>O<sub>4</sub> based ferrofluids were prepared by chemical co-precipitation method as detailed elsewhere<sup>17</sup>. The SPIONs (Fe<sub>3</sub>O<sub>4</sub> nanoparticles having size ~10 nm) coated with citric acid organic hull were dispersed in distilled water by extensive sonication to yield 0.1 g/ml SPION solution. This stable Fe<sub>3</sub>O<sub>4</sub> suspension was used to interact with collagen fibers. Collagen waste in the form of dry hide powder was reacted with SPION solution (0.1 g/ml) in the ratio of 100:50 by a simple room temperature mixing for 2 h using water (2000% based on the weight of collagen) as the medium to obtain magnetic nanobiocomposites. In a typical experiment, 1 g of hide powder was mixed with 20 ml water and further treated with 0.5 g SPION (5 ml of 0.1 g/ml SPION solution) for 2 h at room temperature with magnetic stirring. The reaction mixture was filtered to separate magnetic nanobiocomposites from solvent. It was dried and then stored. Collagen-SPION magnetic nanobiocomposites were used to selectively remove oil from oil-water mixture and track them under magnetic field. Two oils were chosen namely premium motor oil and used motor oil in order to assess the oil absorbing capability of the derived magnetic nanobiocomposites. For each oil selected, a known excess weight (25 g) of oil was placed in a 50 mL beaker and 1 g of magnetic nanobiocomposite was immersed in the oil at room temperature. After specific time intervals (0.17, 1, 2, 15, 30, 45 and 60 min), the amount of oil absorbed by the composite was determined by subtracting the initial composite weight from the total weight of the oil absorbed composite. The premium motor oil absorbed magnetic nanobiocomposite was transferred to a horizontal Quartz reactor and purged with high purity Argon gas at a flow rate of 25 ml/min for 10 min. After purging, the reactor was heated at a heating rate of 10°C/min to 1000°C and held at that temperature for 2 h. After the reaction, the temperature was gradually stepped down to room temperature under the same Argon atmosphere. The volatile products were carried away from the reactor by the continuous flow of Argon gas.

**Characterization of the materials.** Differential scanning calorimetric (DSC) analysis of wet collagen-SPION nanobiocomposite and wet collagen fibers were carried out using TA instruments (Q600 simultaneous TGA/DSC). The heating rate was maintained constant at 2°C/min. The wet nanobiocomposite samples were dehydrated gradually using acetone and methanol for electron microscopic analyses. SEM analysis was carried out using a FEI-Quanta (400F) instrument after gold sputter coating for 60 s. X-ray diffractogram of the pristine collagen waste, nanobiocomposite and carbon materials were obtained using a Rigaku diffractometer, operating with CuK $\alpha$  radiation ( $\lambda = 0.15406$  nm) generated at a voltage of 30 kV and current of 20 mA at a scan rate of 3° per min. The Raman spectra of pristine collagen waste and nanobiocomposite fibers were obtained with a Renishaw InVia laser Raman microscope using a  $\times 50$  objective lens at 785 nm in the range of 800–1800 cm<sup>-1</sup>, with a collection time of 120 s and an accumulation of 3 scans. Raman spectrum of derived carbon was obtained using a 632.8 nm (He-Ne) laser beam and 1,800 lines per mm grating. TEM analysis of nanobiocomposite (dehydrated sample) and derived carbon (sonicated in ethanol) were carried out in a holey carbon grid using a JEOL 2100 Field Emission Gun TEM. XPS analysis was carried out on a PHI Quantera X-Ray photoelectron spectrometer with a chamber pressure of  $5 \times 10^{-9}$  torr and an Al cathode as the X-ray source. The source power was set at 100 W, and pass energies of 140.00 eV for survey scans and 26.00 eV for core-level scans were used. The electrical resistance of the formed carbon materials was measured using a multimeter. Room temperature magnetic measurements on the magnetic nanobiocomposite and as-prepared carbon sample were measured using a SQUID magnetometer (Quantum Design Magnetic Property Measuring System).

- Balazs, A. C., Emrick, T. & Russell, T. P. Nanoparticle polymer composites: where two small fields meet. *Science* **314**, 1107–1110 (2006).
- Olsson, R. T. *et al.* Making flexible magnetic aerogels and stiff magnetic nanopaper using cellulose nanofibrils as templates. *Nat. Nanotechnol.* **5**, 584–580 (2010).
- Mauter, M. S. & Elimelech, M. Environmental applications of carbon-based nanomaterials. *Environ. Sci. Technol.* **42**, 5843–5859 (2008).
- Sinani, V. A. *et al.* Collagen coating promotes biocompatibility of semiconductor nanoparticles in stratified LBL films. *Nano Lett.* **3**, 1177–1182 (2003).
- Lewinski, N., Colvin, V. & Drezek, R. Cytotoxicity of nanoparticles. *Small* **4**, 26–49 (2008).
- Jain, T. K., Reddy, M. K., Morales, M. A., Leslie-Pelecky, D. L. & Labhasetwar, V. Biodistribution, clearance, and biocompatibility of iron oxide magnetic nanoparticles in rats. *Mol. Pharmacol.* **5**, 316–327 (2008).
- Narayanan, T. N. *et al.* Enhanced bio-compatibility of ferrofluids of self-assembled superparamagnetic iron oxide-silica core-shell nanoparticles. *J. Nanosci. Nanotechnol.* **11**, 1958–1967 (2011).
- Ramachandran, G. N. & Kartha, G. Structure of collagen. *Nature* **176**, 593–595 (1955).
- Rao, J. R., Thanikaivelan, P., Sreeram, K. J. & Nair, B. U. Green route for the utilization of chrome shavings (chromium-containing solid waste) in tanning industry. *Environ. Sci. Technol.* **36**, 1372–1376 (2002).
- Sundar, V. J., Gnanamani, A., Muralidharan, C., Chandrababu, N. K. & Mandal, A. B. Recovery and utilization of proteinous wastes of leather making: a review. *Rev. Environ. Sci. Technol.* **10**, 151–163 (2011).
- Thanikaivelan, P., Geetha, V., Rao, J. R., Sreeram, K. J. & Nair, B. U. A novel chromium-iron tanning agent: cross-fertilization in solo tannage. *J. Soc. Leather Technol. Chem.* **84**, 82–87 (2000).
- Chakravorty, H. P. & Nursten, H. E. Uncommon inorganic tannages. *J. Soc. Leather Technol. Chem.* **42**, 2–22 (1958).
- Convington, A. D. Modern tanning chemistry. *Chem. Soc. Rev.* **26**, 111–126 (1997).
- Mo, X., An, Y., Yun, C. S. & Yu, S. M. Nanoparticle-assisted visualization of binding interactions between collagen mimetic peptide and collagen fibers. *Angew. Chem. Int. Edit.* **45**, 2267–2270 (2006).
- Sisco, P. N., Wilson, C. G., Mironova, E., Baxter, S. C., Murphy, C. J. & Goldsmith, E. C. The effect of gold nanorods on cell-mediated collagen remodeling. *Nano Lett.* **8**, 3409–3412 (2008).
- Mary, A. P. R., Narayanan, T. N., Sunny, V., Kumar, D. S. & Anantharaman, M. R. Synthesis of bio-compatible SPION based aqueous ferrofluids and evaluation of radio frequency power loss for magnetic hyperthermia. *Nanoscale Res. Lett.* **5**, 1706–1711 (2010).
- Narayanan, T. N., Mary, A. P. R., Shaijumon, M. M., Ci, L., Ajayan, P. M. & Anantharaman, M. R. On the synthesis and magnetic properties of multiwall carbon nanotube-superparamagnetic iron oxide nanoparticle nanocomposites. *Nanotechnology* **20**, 055607 (2009).
- Casula, M. F. *et al.* Magnetic resonance imaging contrast agents based on iron oxide superparamagnetic ferrofluids. *Chem. Mater.* **22**, 1739–1748 (2010).
- Yuan, J. *et al.* Superwetting nanowire membranes for selective absorption. *Nat. Nanotechnol.* **3**, 332–336 (2008).
- Wang, G., Sun, Q., Zhang, Y., Fan, J. & Ma, L. Sorption and regeneration of magnetic exfoliated graphite as a new sorbent for oil pollution. *Desalination* **263**, 183–188 (2010).
- Adebajo, M. O., Frost, R. L., Klopogge, J. T., Carmody, O. & Kokot, S. Porous materials for oil spill cleanup: a review of synthesis and absorbing properties. *J. Porous Mat.* **10**, 159–170 (2003).
- Jang, J. & Kim, B. S. Studies of crosslinked styrene-alkyl acrylate copolymers for oil absorbency application. I. Synthesis and characterization. *J. Appl. Polym. Sci.* **77**, 903–913 (2000).
- Ceylan, D., Dogu, S., Karacik, B., Yakan, S. D., Okay, O. S. & Okay, O. Evaluation of butyl rubber as sorbent material for the removal of oil and polycyclic aromatic hydrocarbons from seawater. *Environ. Sci. Technol.* **43**, 3846–3852 (2009).
- Choi, S. J. *et al.* A polydimethylsiloxane (PDMS) sponge for the selective absorption of oil from water. *ACS Appl. Mater. Interfaces*; DOI: 10.1021/am201352w.
- Oh, Y. S., Maeng, J. & Kim, S. J. Use of microorganism-immobilized polyurethane foams to absorb and degrade oil on water surface. *Appl. Microbiol. Biotechnol.* **54**, 418–423 (2000).
- Gammoun, A. *et al.* Separation of motor oils, oily wastes and hydrocarbons from contaminated water by sorption on chrome shavings. *J. Hazard. Mater.* **145**, 148–153 (2007).
- Zhu, Q., Tao, F. & Pan, Q. Fast and selective removal of oils from water surface via highly hydrophobic core-shell Fe<sub>2</sub>O<sub>3</sub>@C nanoparticles under magnetic field. *ACS Appl. Mater. Interfaces* **2**, 3141–3146 (2010).
- Zhang, J. & Seeger, S. Polyester materials with superwetting silicone nanofilaments for oil/water separation and selective oil absorption. *Adv. Funct. Mater.*; DOI: 10.1002/adfm.201101090.
- Pagliari, M. & Ciriminna, R. New fluorinated functional materials. *J. Mater. Chem.* **15**, 4981–4991 (2005).
- Sreeram, K. J. & Ramasami, T. Sustaining tanning process through conservation, recovery and better utilization of chromium. *Resour. Conserv. Recy.* **38**, 185–212 (2003).
- Fan, H., Shi, B., He, Q. & Peng, B. Tanning characteristics and tanning mechanism of nano-SiO<sub>2</sub>. *J. Soc. Leather Technol. Chem.* **88**, 139–142 (2004).
- Wu, B., Mu, C., Zhang, G. & Lin, W. Effects of Cr<sup>3+</sup> on the structure of collagen fiber. *Langmuir* **25**, 11905–11910 (2009).
- Weiner, S., Kustanovich, Z., Gil-Av, E. & Traub, W. Dead sea scroll parchments: unfolding of the collagen molecules and racemization of aspartic acid. *Nature* **287**, 820–823 (1980).
- Hulmes, D. J., Jesior, J. C., Miller, A., Colominas, C. B. & Wolff, C. Electron microscopy shows periodic structure in collagen fibril cross sections. *Proc. Natl. Acad. Sci. USA* **78**, 3567–3571 (1981).
- Bigi, A., Fichera, A. M., Roveri, M. & Koch, M. H. J. Structural modifications of air-dried tendon collagen on heating. *Int. J. Biol. Macromol.* **9**, 176–180 (1987).
- Gayatri, R., Sharma, A. K., Rajaram, R. & Ramasami, T. Chromium(III)-induced structural changes and self-assembly of collagen. *Biochem. Biophys. Res. Commun.* **283**, 229–235 (2001).
- Loke, W. K. & Khor, E. Validation of the shrinkage temperature of animal tissue for bioprosthetic heart valve application by differential scanning calorimetry. *Biomaterials* **16**, 251–258 (1995).
- Moll, J. S. & Use, C. J. Water pollution trap and methods of use thereof. *US Patent 7820040* (2010).
- DiLeo, R. A., Landi, B. J. & Raffaele, R. P. Purity assessment of multiwalled carbon nanotubes by Raman spectroscopy. *J. Appl. Phys.* **101**, 064307 (2007).



40. Maultzsch, J. *et al.* Raman characterization of boron-doped multiwalled carbon nanotubes. *Appl. Phys. Lett.* **81**, 2647 (2002).
41. Bersani, D., Lottici, P. P. & Montenero, A. Micro-Raman investigation of iron oxide films and powders produced by sol-gel syntheses. *J. Raman Spectrosc.* **30**, 355–360 (1999).
42. Thanikaivelan, P., Rao, J. R., Nair, B. U. & Ramasami, T. Zero discharge tanning: a shift from chemical to biocatalytic leather processing. *Environ. Sci. Technol.* **36**, 4187–4194 (2002).
43. Saravanabhavan, S., Aravindhan, R., Thanikaivelan, P., Rao, J. R. & Nair, B. U. Green solution for tannery pollution: effect of enzyme based lime-free unhairing and fibre opening in combination with pickle-free chrome tanning. *Green Chem.* **5**, 707–714 (2003).

## Acknowledgements

P.T. thank USIEF, India for the Fulbright-Nehru Senior Research Fellowship that enabled his stay at Rice University, Houston. T.N.N. and P.M.A. acknowledge the financial support from Nanoholdings LLC, Rowayton, Connecticut.

## Author contributions

P.T. and N.T.N. contributed equally to this work. P.T. and N.T.N. designed and carried out most of the experiments (wet chemistry, DSC, XRD, Raman, SEM, TEM, XPS, SQUID, oil removal, heat treatment for carbon preparation), and analysed the data. P.T., B.K.P. and P.M.A. were responsible for the project planning. P.T., N.T.N. and P.M.A. co-wrote the paper. All the authors discussed the results.

## Additional information

**Supplementary information** accompanies this paper at <http://www.nature.com/scientificreports>

**Competing financial interests:** The authors declare no competing financial interests.

**License:** This work is licensed under a Creative Commons Attribution-NonCommercial-ShareAlike 3.0 Unported License. To view a copy of this license, visit <http://creativecommons.org/licenses/by-nc-sa/3.0/>

**How to cite this article:** Thanikaivelan, P., Narayanan, N.T., Pradhan, B.K. & Ajayan, P.M. Collagen based magnetic nanocomposites for oil removal applications. *Sci. Rep.* **2**, 230; DOI:10.1038/srep00230 (2012).